Accepted Article

Title: The Role of a Double Molecular Anchor on the Mobility and Self-Assembly of Thiols on Au(111): the Case of Mercaptobenzoic Acid

Authors: Miriam Candelaria Rodríguez González, Pilar Carro, Evangelina Pensa, Carolina Vericat, Roberto Salvarezza, and Alberto Hernández Creus

ARTICLE

The Role of a Double Molecular Anchor on the Mobility and Self-Assembly of Thiols on Au(111): the Case of Mercaptobenzoic Acid

Miriam C. Rodríguez González [a], Pilar Carro[a], Evangelina Pensa[b.c], Carolina Vericat[b], Roberto Salvarezza[b] and Alberto Hernández Creus*[a]

Abstract: The dynamics of the self-assembly process of thiol molecules on Au(111) is affected by the interplay between molecule-substrate and molecule-molecule interactions. Therefore, it is interesting to explore the effect of a second anchor to the gold surface, in addition to the S atom, on both the order and the feasibility of phase transitions in self-assembled monolayers. To assess the role of an additional O anchor, we have compared the adsorption of two mercaptobenzoic acid isomers, 2-mercaptobenzoic acid (2-MBA) and 4-mercaptobenzoic acid (4-MBA), on Au(111). Results from Scanning Tunneling Microscopy, X-ray Photoelectron Spectroscopy, electrochemical techniques and Density Functional Theory calculations show that the additional O anchor in 2-MBA hinders surface mobility, reducing domain size and impeding the molecular reorganization involved in phase transition to denser phases on the Au(111) substrates. This knowledge can contribute to predict the range order and molecular density of the thiol SAM depending on the chemical structure of the adsorbate.

Introduction

One of the most interesting and basic aspects in the study of self-assembled monolayers (SAMs) of thiols on metal surfaces is their dynamics and the impact that they have in molecular ordering, configuration and phase transitions. It is well-known that the adsorption process results in the formation of ordered molecular domains whose size depends on the temperature, thus reflecting the surface mobility of adsorbed thiol species on the Au(111) surface.[1, 2] It has also been shown that thiol mobility is reduced as van der Waals interactions among adsorbed molecules increase, which results in the decrease of the size of ordered domains, a fact observed for alkanethiols as

a function of the hydrocarbon chain length.[3] On the other hand, strong molecular reorganizations take place during alkanethiol adsorption, leading to a phase transition from diluted lying-down phases to denser standing up phases, usually the well-known $c(4\times2)$ and/or $(\sqrt{3}\times\sqrt{3})R30°$ lattices, with surface coverage $\theta = 0.33$ and a tilt angle (α) ~ $30°$ with respect to the substrate normal.[3, 4] In fact, the system decreases its surface free energy by incorporating more molecules and replacing molecule-substrate interactions by molecule-molecule interactions. A similar situation has been reported for small aromatic thiols and amino acids.[5] Indeed, benzenethiol adsorbs at a low coverage in a nearly parallel configuration forming RS-Au_{ad}-SR moieties (Au_{ad} = adatom, RS= thiol)[6] and tilted $80°$ with respect to the substrate normal.[7] As expected, by increasing adsorption time and/or concentration/pressure, molecules adopt a standing up configuration with a much smaller α value ranging from $19°$ to $30°$,[8-10] which allows to accommodate more molecules to form denser stable structures ($\theta = 0.2$-0.3) via molecule-molecule interactions. However, in contrast to alkanethiols, short aromatic thiols exhibit more disorder, a fact that has been assigned to the strong π–π stacking interaction of the phenyl ring, which leads to a lower surface mobility of thiol/Au complexes and lower surface coverage.[11, 12] On the other hand, the effect of molecule-substrate interactions on molecular order has been revealed from the study of 2-mercaptoimidazole, 2-mercaptobenzothiazole, 2-mercaptobenzoxazole[13] and 6-mercaptopurine SAMs on Au(111).[14] These molecules adsorb disorderly and are bound to the substrate not only through the thiolate group but also through additional N, S or O heteroatoms. Ordered arrays of molecules parallel to the substrate normal with surface coverage 0.2 are only observed when partial electrochemical desorption occurs.[13]

Therefore, it is interesting to explore the effect that an additional anchor on the Au surface has on molecular order and the feasibility of phase transitions. This knowledge can shed light on how molecules manage energy optimization between molecule-substrate and molecule-molecule interactions in thiol SAMs. We have recently studied 4-mercaptobenzoic acid (4-MBA) SAMs on Au(111) by different techniques.[15, 16] Our results showed that this molecule initially forms ordered domains with a $(4\times\sqrt{3})$ lattice with two molecules per unit cell and surface coverage $\theta = 0.25$ and then undergoes a phase transition to reach $\theta = 0.33$, a figure consistent with the $c(4\times2)$ lattice.[16] On the other hand, 4-MBA adsorbs on the Au(110) from gaseous phase forming dimeric structures nearly parallel to the Au surface forming a (5×4) lattice with $\theta = 0.20$.[17] It means that 4-MBA surface structure is dependent on the Au crystal face.

In the present work we have studied the 2-mercaptobenzoic acid (2-MBA) isomer, which has the possibility

[a]   M. C. Rodríguez González, P. Carro and A. Hernández Creus
       Área de Química Física, Departamento de Química, Facultad de
       Ciencias, Universidad de La Laguna, Instituto de Materiales y
       Nanotecnología, 38200-La Laguna, Tenerife, Spain.
       E-mail: ahcreus@ull.edu.es

[b]   E. Pensa, C. Vericat and R. Salvarezza
       Instituto de Investigaciones Fisicoquímicas Teóricas y Aplicadas
       (INIFTA), Facultad de Ciencias Exactas, Universidad Nacional de
       La Plata - CONICET- Sucursal 4 Casilla de Correo 16, (1900) La
       Plata, Argentina.

[c]   E. Pensa
       Author Present Address EP Imperial College London, Department of
       Chemistry, Exhibition Road SW7 2AZ, UK

to interact with the Au(111) surface through the O atoms of the carboxylate group in the ortho position. We have found that the O-Au interaction, which in principle should be relatively weak,[13] hinders molecule mobility, thus increasing surface disorder and impeding the molecular reorganization involved in phase transition to denser phases. In our best knowledge, it is the first time that such a strong effect on thiol SAMs properties is reported as a result of an additional O-substrate interaction.

Results and Discussion

STM images of the Au(111) surface after 2-MBA adsorption (Figure 1a) show atomically smooth terraces separated by steps of monatomic height (0.24 nm) (Figure 1c), without any evidence of vacancy island formation. On the other hand, in some areas of the Au(111) substrates nanometer sized islands are observed (bright spots in Figure 1b) whose height is well below 0.24 nm (~0.11 nm), thus indicating that they correspond to molecular agglomerates, as reported for other aromatic thiols on Au(111).[18] The darker regions in this image can be associated with pinholes, as their depth is smaller than 0.24 nm. STM images at higher resolution reveal small domains (< 20 nm) of ordered rows coexisting with disordered regions (Figure 1d).
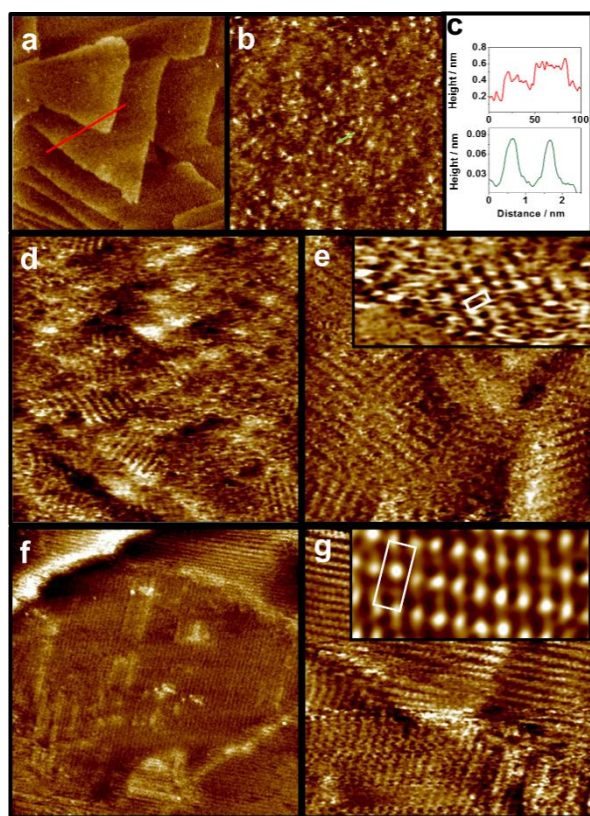

Figure 1. In air high resolution STM images and related data. (a) 2-MBA SAM on Au(111) showing terraces and steps (200×200 nm^2). (b) A disordered region of a 2-MBA SAM showing molecular aggregates (20×20 nm^2). c) Cross-

sectional analysis of the segments in images a) and b). Upper: monatomic high steps (0.24 nm); lower: molecular aggregates (0.1 nm). d) 2-MBA SAM showing ordered and disordered domains coexisting on the Au(111) surface (50×50 nm^2). e) Ordered domains of the 2-MBA SAM showing rows of molecules (30×30 nm^2). f) Ordered domains of the 4-MBA SAM on Au(111) (50 × 50 nm^2). (g) Ordered domains of 4-MBA SAM showing rows of molecules (20×20 nm^2). Insets in Figures e) and g) show details of the molecular arrays. Unit cells are indicated.

Rows are separated by 1.2±0.05 nm and intersect the substrate steps with 60º or 120° angles, therefore revealing the influence of the substrate orientation (Figure 1e). Although some spots inside the rows with ∼ 0.5 nm nearest neighbor distances were detected, it was not possible to obtain better resolution. Similar STM images taken on 4-MBA covered substrates show larger domains, which can reach 50 nm in size (Figure 1f), consisting of molecular rows separated by 0.69±0.02 nm. In this case 4-MBA molecules are clearly observed within each row, separated by 0.47±0.02 nm (Figure 1g), yielding the well-known (4×√3) lattice with with a surface coverage $\theta = 0.25$ that has been observed for different aromatic thiols.[15, 16, 18]

In order to estimate the surface coverage of the 2-MBA on the Au(111) surface we have performed reductive desorption measurements.[19] Typical electroreduction curves of 2-MBA SAMs on Au(111) yield a small peak with a peak potential $E_p = -0.47$ V (Figure 2, full red line). The charge density (q) involved in the peak at -0.47 V is q =25±7 μC cm^{-2}. Taking into account that thiol reductive desorption is a one-electron process, and considering the surface density of gold atoms on the Au(111) surface, a thiol coverage $\theta = 0.11$ is obtained.
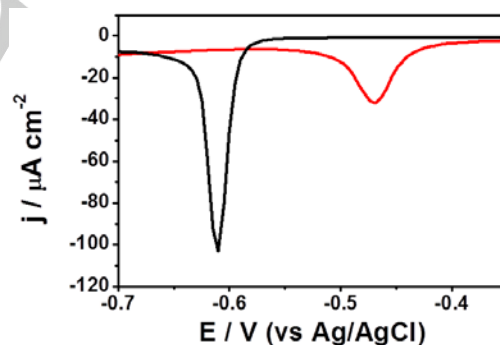
Figure 2. Electrodesorption curves for 2-MBA (red) and 4-MBA SAMs (black) on Au(111).

Therefore, based on this result and on the STM images (Figures 1d-e), we can assign the ordered domains of 2-MBA molecules to the same (4×√3) lattice but with $\theta = 0.12$. In contrast, the 4-MBA reductive desorption from the Au(111) surface originates a sharp peak at -0.62 V involving q = 55±7 μC cm^{-2}, and accordingly, $\theta = 0.24$. The larger q value, the sharper peak and the shift of E_p toward negative potentials[20] (Figure 2, black line) are all consistent with a denser, more ordered, and more stable 4-MBA SAM compared to that for 2-MBA.

There is also another important difference in the time evolution of these SAMs. Indeed, for 4-MBA larger immersion times (typically 24 h) and/or higher concentrations of the solutions lead to a significant increase in the charge density to q = 75±7 μC cm^{-2}, which results in θ = 0.33, a value consistent with the c(4×2) surface structure[16], and therefore, with the tilt angle α = 30° obtained from XANES data measured under these experimental conditions.[21] This behavior, however, has not been observed for 2-MBA SAMs, whose surface coverage is 0.11 irrespective of immersion time and solution concentration.

Therefore, the main differences between 4-MBA and 2-MBA SAMs on Au(111) are the size of the ordered domains and the surface coverage, including their time evolution. While 4-MBA can form larger and denser molecular domains (Figure 1f-g), 2-MBA yields smaller and more diluted ordered molecular domains that coexist with disordered regions (Figure 1d-e). Domains 10 nm in size were also observed for mercaptobenzoxazole on Au(111) and attributed to the weak O-Au interaction that prevents molecular ordering.[13]

Figure 3 shows high resolution XP spectra for 2-MBA (lower) and 4-MBA (upper) SAMs on Au(111). For both samples the Au 4f region can be fitted with one component with Au4f$_{7/2}$ BE = 84.0 eV (Figure 3a), which corresponds to metallic gold. The S 2p region can be also fitted with a single component with S 2p$_{3/2}$ BE = 162.0 eV (Figure 3b), attributed to the formation of a thiolate bond on Au(111). The S/Au signal ratio confirms the electrochemical and STM data showing that the surface coverage of 4-MBA is twice that obtained for the 2-MBA.

Larger C/S and O/S ratios were found for 2-MBA, a fact that can be explained considering the lower coverage of 2-MBA SAMs. Therefore, the contribution from physisorbed species arising from the exposure to the atmosphere during transfer to the UHV chamber and also probably the adsorption of some solvent molecules sample is considerable for 2-MBA SAMs, while it is markedly reduced in the denser 4-MBA SAMs.
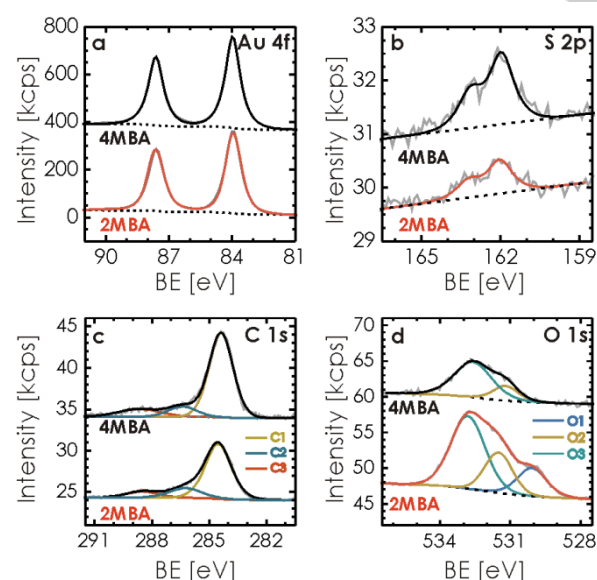
Figure 3. High resolution XP spectra for 2-MBA (lower, red line) and 4-MBA (upper, black line). a) Au 4f, b) S 2p, c) C 1s, d) O 1s. 4-MBA spectra were vertically shifted for clarity.

Three components were needed to correctly fit the C 1s signal (Fig 3c). The main component, C1, at ~ 284.5 eV, is assigned to C atoms in the aromatic ring,[22, 23] and in the case of 2-MBA there is some additional contribution from adventitious C (C-H) from the atmosphere. Component C2 (~ 286.3 eV) can be assigned to the C atoms adjacent to the S and carboxylate groups[7, 24] (with probably some contribution from ethanol molecules[25]), while component C3 (~ 288.5 eV) corresponds to carboxylate groups[22, 24]. The C3/S ratio is at least 20% larger for 4-MBA than for 2-MBA, suggesting a more external location of this group in the 4-MBA SAM.

Finally, a broad O 1s spectrum is observed for both SAMs (Figure 3d). For 4-MBA there are two different states for oxygen, O1 and O2, with binding energies ~532.7 eV and ~531.4 eV, respectively. The first component O1 can be related to the carboxyl of the neutral species while O2 corresponds to the oxygen atoms of the electronically delocalized carboxylate species.[26] For 2-MBA, in addition to the aforementioned components, there is a third component O3 at BE ~ 530.1 eV which can be assigned to the carboxylate group that interacts with the gold surface.[22, 27]

Therefore, in agreement with previous results from C K-edge NEXAFS experiments of the MBA isomers on Au(111),[21] XPS data confirm that 4-MBA molecules are chemisorbed on the Au(111) surface through the S atom, with the COOH group at the outer part of the SAM, while 2-MBA molecules are bound to the substrate through both the S and the O atoms from the carboxylate group.

We have modeled the rectangular 1.2 nm×0.5 nm 2-MBA surface structures observed in the STM images as a (p×√3) lattice with coverage θ = 0.125. Three different models have been considered: one with the protonated carboxylate group (model A) (Figure 4a), and two with deprotonated carboxylate groups, models B (Figure 4b) and C (Figure 4c).

In models A and B (Figures 4a and 4b) the surface structure can be described by a (4×√3) unit cell with one 2-MBA radical or diradical, respectively, and distances between adjacent S heads of 0.12 nm and 0.51 nm in the x and y directions, in good agreement with STM images. In model A the 2-MBA moiety is bonded to the Au(111) surface only through the S atom, which is placed at a bridge position (the COOH group is far from the Au(111) surface), and the molecular tilt angle α is 50° (Figure 4a, inset). The E_b value is -2.49 eV, very close to the -2.56 eV calculated for the 4-MBA (Table 1). It should be noted that in model A, 2-MBA stands for a radical with a deprotonated thiol group and a protonated carboxylic group. This configuration would correspond to 2-MBA molecules in disordered regions where the COOH could not be interacting with the Au(111) surface.

On the other hand, in the optimized structure for model B (Figure 4b) the 2-MBA moiety is bonded not only through S atom at bridge sites but also by O atoms, interacting at near on-top sites of the Au(111) surface (Figure 4b). The additional anchor has a strong effect on the E_b value that increases to -3.02 eV,

thus adding 0.53 eV for the two O atom-Au interactions (Figure 4b, inset). Note that these interactions only have a slight effect on α, which remains almost constant ($\alpha = 53°$), in good agreement with previous XANES data.[21] Although surface free energy (γ) values reveal that model B is thermodynamically more stable than model A, it is clearly more unstable than the 4-MBA lattice, as the former has half of the surface coverage (0.125 vs 0.25) (Table 1). Thus, as already reported[28, 29], binding energies alone cannot be used to predict the stability of adsorbed layers because of the strong influence of the surface coverage.
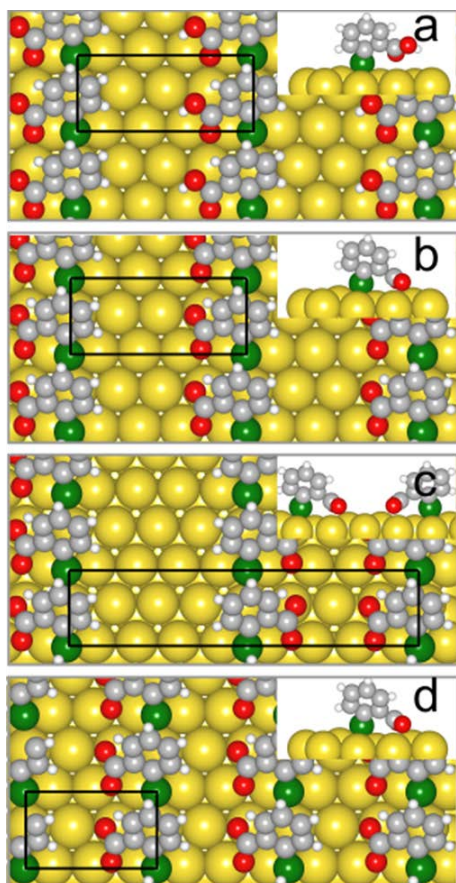
Figure 4. Top and side views of the optimized structures on Au(111) described in the text. a) Model A: (4×√3) 2-MBAH. b) Model B: (4×√3) 2-MBA. C) Model C: (8×√3) 2-MBA. d) Model D: (3×√3) 2-MBA on an unreconstructed Au(111) lattice. Color of the atoms: yellow, Au; green, S; gray, C; white, H; red, O atoms.

Model C represents a (8×√3) unit cell with two 2-MBA molecules in an antiparallel structure with the same surface coverage and similar S and O interactions with the Au(111) surface as in model B. The aim of this model was to analyze the influence of long range interactions on the stability of the surface structure (Figure 4c and inset). Results in Table 1 show that both E_b and γ are similar to those found for model B, and thus both models can be regarded as energetically equivalent.

Table 1. Energetic, structural and Bader charge data for MBA surface structures on Au(111)

	2-MBA$_H$		2-MBA		4-MBA
Surface lattice	Model A (4×√3)	Model B (4×√3)	Model C (8×√3)	Model D (3×√3)	(4×√3)
θ	0.125	0.125	0.125	0.167	0.25
E_b/eV	-2.49	-3.02	-2.95	-3.00	-2.56
γ/meV/Å^2	-41.59	-50.38	-49.26	-66.83	-85.0
Bader Charge/e — S	-0.07	-0.07	-0.06	-0.06	-0.11
Bader Charge/e — O	-	-1.70	-1.71	-1.72	-
Bader Charge/e — Au	+0.06	+0.06(S) +0.14(O)	+0.07(S) +0.16(O)	+0.08(S) +0.14(O)	+0.05
z(S-Au)/Å	1.95	1.97	1.94	1.99	2.0
z(O-Au)/Å	-	2.06	2.08	2.1	-
α/degrees	50.6	53.0	49.1	49.6	46.1
$\Delta\Phi$/eV	-1.0	-0.47	-0.50	-0.61	-0.19

It should be noted that the difference between the γ values of models B and C for 2-MBA and that corresponding to the model for 4-MBA (Table 1) fairly accounts for the large difference in E_p values observed in the reductive desorption curves (Figure 2). In fact, while O-Au interactions add 0.5 eV to the S-Au bond, the number of thiolates is significantly smaller for the 2-MBA SAM compared to a 4-MBA SAM (θ = 0.125 vs θ = 0.25), thus resulting in smaller γ values (equation 2) and thus in a smaller stability.

The Bader charge analysis of models B and C reveals that the negative charge is accumulated on the S and O atoms and, accordingly, positive charges are accumulated on the underlying Au atoms, with the largest negative charge and positive charges present on the O and the Au atom beneath it, respectively. The charge density difference isosurfaces of (4×√3)-2-MBA/Au(111) (model B) show the charge density accumulation after adsorption more clearly (Figure 5a). The simulated STM images of model B (Figure 5b) are fairly in agreement with the experimentally observed rows of 2-MBA molecules (Figure 1e).
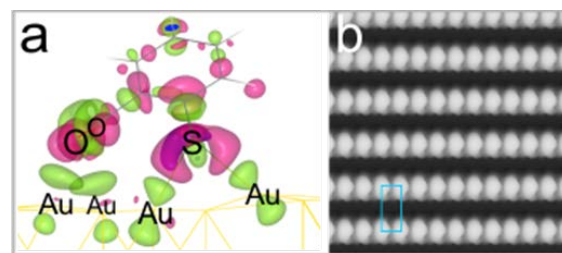

Figure 5. a) Charge density difference isosurfaces for the 2-MBA (4×√3) lattice on Au(111) (model B) showing electronic charge accumulation (pink) and depletion (green). b) Simulated STM image of model B. The (4×√3) unit cell with dimensions 5.09 Å×11.8 Å is shown.

We have performed O 1s core level shift (CLS) calculations for 2-MBA in model B and 4-MBA on Au(111). Results show that when the O atoms are in contact with the Au surface (2-MBA surface structure), the O 1s BE is expected to be shifted to smaller values by about 1.4 eV with respect to the non-interacting O atoms (as in the 4-MBA surface structure).

This result supports our interpretation of the 530 eV component in the O 1s XPS spectra in Figure 3.

It is also interesting to analyze the role of the surface dipoles of the SAMs by comparing the changes in the calculated work function $\Delta\Phi$ for the models studied in this work (Table 1). It is known that $\Delta\Phi$ is related to the change in the vertical component of the adsorbate dipole upon adsorption, $\Delta\mu_{\perp}$.[30] The position of the carboxylate group in the phenyl ring dramatically modifies the adsorbate dipoles and this is reflected in the difference in $\Delta\Phi$ between the two isomers. Indeed, $\Delta\Phi$ values for 2-MBA, either model B (-0.47 eV) or C (-0.5 eV), are larger than that for 4-MBA (-0.19 eV) due to the larger molecular dipole of the 2-MBA isomer. On the other hand, when comparing 2-MBA models, B and C present smaller $\Delta\Phi$ than model A, due to the presence of larger surface dipoles with their directions opposite to the molecular dipole in models B and C. In fact, models B and C bind to the surface through O-Au and S-Au bonds, while model A, which has the protonated carboxylate group, only binds to the surface through the S-Au bond.

Now we will discuss why 2-MBA and 4-MBA SAMs reach different surface coverage values on the same surface. It seems evident that the π- π interaction between the phenyl ring of adjacent molecules and that of π electrons with the Au surface are responsible for the molecular tilt, as no significant differences are found in α values whether O interacts or not with the Au surface (models B-C and A, respectively). Also, because 2-MBA and 4-MBA have similar α values, the aromatic ring–Au surface interactions should be of similar magnitude. Thus, in order to understand the differences in surface coverage between both adsorbates, it becomes necessary to compare the respective molecular shapes and their projected areas. Figure 6 shows that the average projected area of a 2-MBA molecule on the substrate is ∼ 30 Å^2, a figure twice the value for a 4-MBA molecule (∼ 15 Å^2). This difference is a consequence of the lateral position of the carboxylate group in the 2-MBA molecule, as it can be seen in Figure 6 (shadowed area).
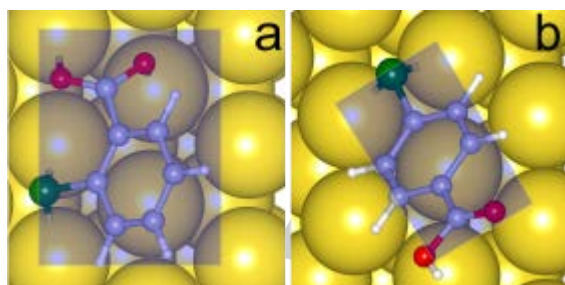

Figure 6. Projected areas for a) 2-MBA and b) 4-MBA molecules on Au(111) .

But is this difference in the projected molecular area responsible of the fact that 2-MBA does not reach a larger surface coverage as 4-MBA does on Au(111)? STM and electrochemical data reveal that the surface coverage of 2-MBA on Au(111) is neither time nor concentration dependent, in contrast to what occurs for 4-MBA, which presents a phase transition from the (4×√3) structure (θ =0.25, α = 46°) to a c(4×2) lattice (θ = 0.33, α = 30°)[16],[21]

by increasing either immersion times or MBA concentration in solution. In order to answer this question we have built a hypothetical (3×√3) model for 2-MBA (model D in Table 1, Figure 4d) with θ = 0.17 and a similar tilt angle (α = 49°). This surface model exhibits the same binding energy (E_b= -3.00 eV) but a better stability (γ = -66.83 meV A^{-2}), thus discarding the role of repulsive interactions to hinder the phase transition towards denser 2-MBA layers. Also, this difficulty is not related to changes in the molecule tilt angle, as models B, C and D have all similar α values (Table 1).

Therefore, we can speculate that the O-Au interaction introduces an extra energy barrier that impedes the reorganization of 2-MBA needed to incorporate more molecules to form denser phases. In order to explore this possibility we have calculated the energy barriers along the diffusion path of a 2-MBA molecule involved when going from model B ((4×√3), θ = 0.125) to model D ((3×√3), θ = 0.17). In this case the adsorbed 2-MBA molecule has to diffuse on the Au(111) surface between two neighbor bridge sites (1 and 4 Figure 7, top panel).
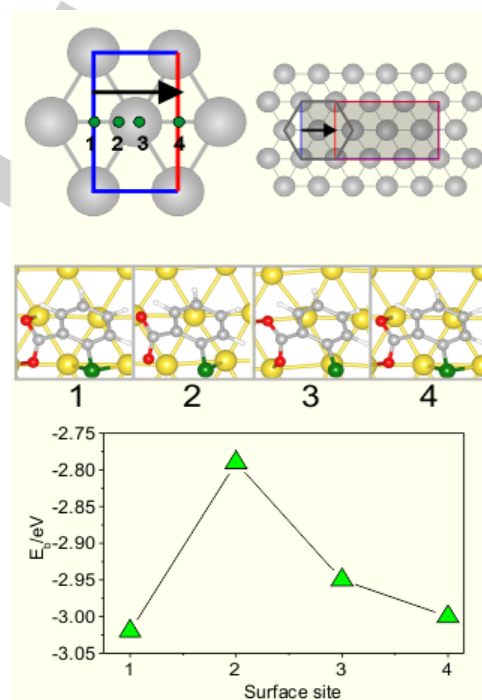
Figure 7. Top panel: Four trajectories of 2-MBA on the Au(111) surface to transform the (4×√3) lattice into the hypothetical (3×√3) lattice. Middle panel: Optimized structures in each point. Bottom panel: E_b values along the trajectory (1-4).

The most direct way to accomplish this task is by hopping the Au atom between these sites. Thus, we have calculated the E_b values in points 2 and 3 in Figure 7, top panel. The optimized geometries in each site are very similar in all cases but it is important to outline that the sulfur atom in sites 2 and 3 are single bonded to the Au surface, in contrast with the most stables geometries in 1 and 4, where S is double-bonded (bridge

sites) to the surface Au atoms. Besides, in site 2 (the one with the least binding energy), one of the O atom cannot be bonded to the surface. Therefore, the binding energy difference between sites 2 and 1 sets up a barrier height of 0.23 eV (Figure 7, middle panel), i.e. a value that is higher than for aromatic thiols bearing only the thiolate anchor to gold, which exhibit small activation energies for translation (0.15-0.19 eV).[31] One can conclude that even this relatively small energy barrier resulting from the partial de-coordination of O and S atoms from the surface hinders molecule reorganization and the formation of a denser phase. Thus, the blocking effect can be assigned to the more limited surface diffusion for a molecule with two atoms anchors to the substrate.[32, 33],[34]

Conclusions

We have found that the oxygen-metal interaction in adsorbed thiolates on Au(111) have marked effects in the SAM structure and evolution. The O-metal interaction introduces additional energy barriers for surface diffusion that result in molecular disorder, smaller domain size and also hinder the formation of denser phases.

Experimental Section

SAM formation

2-MBA (Aldrich 97%) and 4-MBA (Aldrich 99,99%) were self-assembled on preferred oriented Au(111) substrates prepared by flame annealing of evaporated Au on chromium-coated glass plates (Arrandee™). Substrates were immersed in 10^{-4} M thiol-containing ethanolic solutions for 1-2 h. In the case of 2-MBA, samples incubated for longer times (up to 40 h) and in solutions of higher concentrations (10^{-3} M) were also studied. In all cases the modified substrates were carefully rinsed with ethanol and dried under N_2.

Scanning Tunneling Microscopy (STM)

STM images in the constant current mode were taken with a Nanoscope IIE (Digital Instruments/Bruker) operating in air at room temperature by using either commercial Pt/Ir or electrochemically etched W tips. Typical tunneling currents (i_t), applied bias voltages (V_{bias}) and scan rates were 0.15-0.4 nA, -0.6 to +1 V, and 0.5-10 Hz, respectively. The calibration of the scanner in the x,y-directions was checked by imaging highly oriented pyrolytic graphite (HOPG) with atomic resolution, while for the z-direction monatomic Au steps were used.

X-Ray Photoelectron Spectroscopy (XPS)

X-Ray photoelectron spectroscopy was conducted on a Thermo Scientific K-alpha spectrometer with monochromated Al Kα radiation, a dual beam charge compensation system and constant pass energy of 20 eV. Survey scans were collected in the binding energy (BE) range 0–1200 eV. The BE scale was calibrated by setting the Au $4f_{7/2}$ BE to 84.0 eV with respect to the Fermi level.

High resolution spectra were fitted with XPS Peak v 4.1 software. Either Shirley or linear type backgrounds were used during the fitting procedure and peaks that are a combination of Lorentzian and Gaussian functions were employed for all regions. In the case of the Au 4f (S 2p) signal, the spin-orbit doublet separation was fixed at 3.65 (1.18 eV) and an intensity ratio 4:3 (2:1) was used. Quantitative analysis was performed with

CasaXPS v 2.3.14 software. Atomic concentrations were calculated with the corresponding relative sensitivity factors (RSF).

Electrochemical Measurements

Electrochemical measurements were made with an Autolab PGSTAT30 potentiostat and a three-electrode conventional electrochemical cell. A large area Pt coil was used as counter electrode and a Ag/AgCl electrode was employed as reference electrode (RE). All potentials in the text are referred to this RE. Aqueous 0.1 M NaOH solutions were prepared by using NaOH pellets (Sigma-Aldrich; 99.99 % trace metals basis) and ultrapure water with 18.2 MΩ cm resistivity (Millipore Products, Bedford). Thiol reductive electrodesorption curves were performed at room temperature by scanning the potential from -0.3 to -1.4 at 0.05 Vs^{-1} in the 0.1 M NaOH solutions. In each case the charge density (q) involved in the reductive peak desorption was obtained by integration of the peak area. The total electrode real area was measured through the gold oxide reduction peak after complete electrodesorption of the thiol. The q value and peak potential (E_p) were taken as a measure of the surface coverage and stability of the thiol SAM, respectively.[19]

Computational methods

DFT calculations for 2-MBA structural models on the Au(111) surface were performed by using the periodic plane-wave set code Vienna Ab initio simulation package (VASP 5.2.12) based on density functional theory (DFT)[35, 36]. We have followed the scheme of non-local functional proposed by Dion et al.[37], vdW-DF, and the optimized Becke88 exchange functional optB88-vdW[38] to take into account the van der Waals (vdW) interactions. The electronic wave functions were expanded in a plane-wave basis set with a 450 eV cutoff energy. The projector augmented plane wave (PAW) due to Blöchl method has been used to represent the atomic cores[39] with PBE potential. Gold surfaces were represented by five atomic layers and a vacuum of ~14 Å separates any two successive slabs. Optimal grids of Monkhorst-Pack[40] k-points 9×5×1 (($\sqrt{3}$×4) and ($\sqrt{3}$×3) lattices) and 9×3×1 (($\sqrt{3}$×8) lattice) have been used for numerical integration in the reciprocal space. Surface relaxation is allowed in the three uppermost Au layers of the slab, as well as the atomic coordinates of the adsorbed species were allowed to relax without further constraints. The atomic positions were relaxed until the force on the unconstrained atoms was lesser than 0.03 eV/Å. The adsorbates are placed just on one side of the slab and all calculations include a dipole correction. Radical species 2-MBA* was optimized in an asymmetric box of 24 Å × 24 Å × 26 Å with a spin polarized calculation. The calculated Au lattice constant is 4.16 Å, which compares reasonably well with the experimental value (4.078 Å).[41]

The adsorption of both the radical (which results when the molecule loses the hydrogen atom of the S-H group) and the diradical (when it loses also the hydrogen atom of the carboxylate group [42] has been studied. The average binding energy per adsorbed 2-MBA* (radical or diradical) E_b, is defined in Eq. [1]:

$$E_b = \frac{1}{N_{2-MBA^*}} \left[E_{2-MBA@Au} - E_{Au(111)} - N_{2-MBA^*} E_{2-MBA^*} \right] \quad [1]$$

where $E_{2-MBA@Au}$, $E_{Au(111)}$ and E_{2-MBA^*} stand for the total energy of the adsorbate-substrate system, the energy of the Au slab, and the energy of 2-MBA* radical respectively, whereas N_{2-MBA^*} is the number of 2-MBA* radicals in the surface unit cell. A negative number indicates that adsorption is exothermic with respect to the separate clean surface and 2-MBA*.

The Gibbs free energy of adsorption of the surface structure (γ) was approximated through the total energy from DFT calculations by using equation [2]:

$$\gamma = \frac{N_{2-MBA} * E_b}{A} \quad [2]$$

where A is the unit cell area. Considering that we are concerned with free energy differences, it is reasonable to assume that the contributions coming from the configurational entropy, the vibrations and the work term (pV) can be neglected.[22-23]

The change in the work function ($\Delta\Phi$) caused by SAM formation with respect to the clean Au(111) surface is defined as

$$\Delta\Phi = \Phi_{SAM} - \Phi_{clean} \quad [3]$$

Constant current STM images of the optimized lattices were simulated by using the Tersoff-Hamann method in its most basic form, i.e. with the STM tip approximated as a point source.[43]

In order to determine the O 1s corel level shifts (CLSs) the Janak-Slater approach has been applied where half an electron (1s) O has been excited from the core level to the valence region and placed in the lowest unoccupied orbital.[44]

.

Acknowledgements

Keywords: SAMs • MBA • STM • Surface diffusion • DFT

[1] Z. Suo, Y. F. Gao, G. Scoles, *J. Appl. Mech. Trans. ASME* **2004**, *71*, 24-31.
[2] H. Guesmi, N. B. Luque, E. Santos, F. Tielens, *Chemistry – A European Journal* **2016**, doi:10.1002/chem.201604574.
[3] F. Schreiber, *Prog Surf Sci* **2000**, *65*, 151-256.
[4] C. Vericat, M. E. Vela, G. Benitez, P. Carro, R. C. Salvarezza, *Chem. Soc. Rev.* **2010**, *39*, 1805-1834.
[5] D. Costa, C. Pradier, F. Tielens, L. Savio, *Surf Sci Rep* **2015**, *70*, 449-453.
[6] P. Maksymovych, J. T. Yates Jr., *J. Am. Chem. Soc.* **2008**, *130*, 7518-7519.
[7] C. M. Whelan, C. J. Barnes, C. G. H. Walker, N. M. D. Brown, *Surf. Sci.* **1999**, *425*, 195-211.
[8] L. Wan, M. Terashima, H. Noda, M. Osawa, *J Phys Chem B* **2000**, *104*, 3563-3569.
[9] D. Käfer, A. Bashir, G. Witte, *J. Phys. Chem. C* **2007**, *111*, 10546-10551.
[10] F. P. Cometto, E. M. Patrito, P. Paredes Olivera, G. Zampieri, H. Ascolani, *Langmuir* **2012**, *28*, 13624-13635.
[11] G. Yang, G. Liu, *J Phys Chem B* **2003**, *107*, 8746-8759.
[12] Y. Liu, Y. Lee, *Nanoscale* **2012**, *4*, 2093-2100.
[13] B. Cui, T. Chen, D. Wang, L. Wan, *Langmuir* **2011**, *27*, 7614-7619.
[14] F. Lobo Maza, D. Grumelli, P. Carro, C. Vericat, K. Kern, R. C. Salvarezza, *Nanoscale* **2016**, *8*, 17231-17240.
[15] E. Pensa, A. A. Rubert, G. Benitez, P. Carro, A. G. Orive, A. H. Creus, R. C. Salvarezza, C. Vericat, *J. Phys. Chem. C* **2012**, *116*, 25765-25771.
[16] M. C. R. González, A. G. Orive, P. Carro, R. C. Salvarezza, A. H. Creus, *J. Phys. Chem. C* **2014**, *118*, 30013-30022.
[17] N. Hauptmann, R. Robles, P. Abufager, N. Lorente, R. Berndt, *J. Phys. Chem. Lett.* **2016**, *7*, 1984-1990.
[18] K. Seo, E. Borguet, *J. Phys. Chem. C* **2007**, *111*, 6335-6342.
[19] T. Kakiuchi, H. Usui, D. Hobara, M. Yamamoto, *Langmuir* **2002**, *18*, 5231-5238.
[20] O. Azzaroni, M. E. Vela, H. Martin, A. Hernández Creus, G. Andreasen, R. C. Salvarezza, *Langmuir* **2001**, *17*, 6647-6654.
[21] J. R. I. Lee, T. M. Willey, J. Nilsson, L. J. Terminello, J. J. De Yoreo, T. Van Buuren, *Langmuir* **2006**, *22*, 11134-11141.
[22] H. Aitchison, H. Lu, S. W. L. Hogan, H. Früchtl, I. Cebula, M. Zharnikov, M. Buck, *Langmuir* **2016**, *32*, 9397-9409.
[23] A. Shaporenko, A. Terfort, M. Grunze, M. Zharnikov, *J Electron Spectrosc Relat Phenom* **2006**, *151*, 45-51.
[24] A. Vallée, V. Humblot, R. Al Housseiny, S. Boujday, C. Pradier, *Colloids Surf. B Biointerfaces* **2013**, *109*, 136-142.
[25] Z. Liu, T. Duchon, H. Wang, D. C. Grinter, I. Waluyo, J. Zhou, Q. Liu, B. Jeong, E. J. Crumlin, V. Matolín, D. J. Stacchiola, J. A. Rodriguez, S. D. Senanayake, *Phys. Chem. Chem. Phys.* **2016**, *18*, 16621-16628.
[26] R. T. Seljamäe-Green, G. J. Simpson, F. Grillo, J. Greenwood, S. M. Francis, R. Schaub, P. Lacovig, C. J. Baddeley, *Langmuir* **2014**, *30*, 3495-3501.
[27] I. Cebula, H. Lu, M. Zharnikov, M. Buck, *Chem. Sci.* **2013**, *4*, 4455-4464.
[28] D. Torres, P. Carro, R. C. Salvarezza, F. Illas, *Phys. Rev. Lett.* **2006**, *97*.
[29] D. Costa, M. Smerieri, I. Tranca, L. Savio, L. Vattuone, F. Tielens, *J. Phys. Chem. C* **2014**, *118*, 29874-29879.
[30] P. C. Rusu, G. Brocks, *Phys. Rev. B Condens. Matter Mater. Phys.* **2006**, *74*.
[31] J. Kucera, A. Gross, *Langmuir* **2008**, *24*, 13985-13992.
[32] A. Franke, E. Pehlke, *Phys. Rev. B Condens. Matter Mater. Phys.* **2010**, *82*.
[33] T. Y. B. Leung, M. C. Gerstenberg, D. J. Lavrich, G. Scoles, F. Schreiber, G. E. Poirier, *Langmuir* **2000**, *16*, 549-561.
[34] K. L. Wong, K. Kwon, L. Bartels, *Appl. Phys. Lett.* **2006**, *88*.
[35] G. Kresse, J. Hafner, *Physical Review B* **1993**, *48*, 13115-13118.
[36] G. Kresse, J. Furthmüller, *Comput Mater Sci* **1996**, *6*, 15-50.
[37] M. Dion, H. Rydberg, E. Schröder, D. C. Langreth, B. I. Lundqvist, *Phys. Rev. Lett.* **2004**, *92*, 246401-1.
[38] J. Klimeš, D. R. Bowler, A. Michaelides, *J Phys Condens Matter* **2010**, *22*.
[39] P. E. Blöchl, *Physical Review B* **1994**, *50*, 17953-17979.
[40] H. J. Monkhorst, J. D. Pack, *Physical Review B* **1976**, *13*, 5188-5192.
[41] W. B. Pearson, *Handbook of Lattice Spacing and Structure of Metals*, Pergamon Press, Inc., New York, **1958**.
[42] M. Wells, D. L. Dermody, H. C. Yang, T. Kim, R. M. Crooks, A. J. Ricco, *Langmuir* **1996**, *12*, 1989-1996.
[43] J. Tersoff, D. R. Hamann, *Physical Review B* **1985**, *31*, 805-813.
[44] K. Gotterbarm, N. Luckas, O. Höfert, M. P. A. Lorenz, R. Streber, C. Papp, F. Viñes, H. Steinrück, A. Görling, *J. Chem. Phys.* **2012**, *136*.
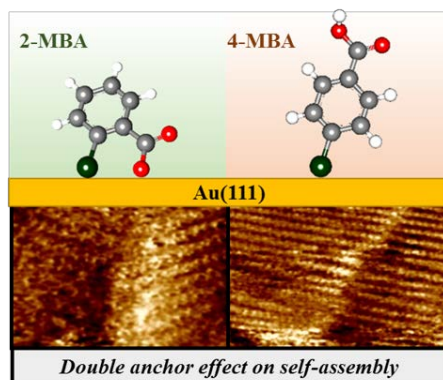
Entry for the Table of Contents (Please choose one layout)

Layout 1:

ARTICLE

To assess the role of an additional O anchor on the order and dynamics of self-assembled monolayers, the mercaptobenzoic acid isomers case, 2-mercaptobenzoic acid (2-MBA) and 4-mercaptobenzoic acid (4-MBA), on Au(111) have been studied.

2-MBA 4-MBA

Au(111)

Double anchor effect on self-assembly

Miriam C. Rodríguez González, Pilar Carro, Evangelina Pensa, Carolina Vericat, Roberto Salvarezza and Alberto Hernández Creus*

Page No. – Page No.

The Role of a Double Molecular Anchor on the Mobility and Self-Assembly of Thiols on Au(111): the Case of Mercaptobenzoic Acid

Layout 2:

ARTICLE

((Insert TOC Graphic here))

Author(s), Corresponding Author(s)*

Page No. – Page No.

Title

Text for Table of Contents